Article

Metal-Free Catalysts for the Hydrolysis of RNA Derived from Guanidines, 2-Aminopyridines, and 2-Aminobenzimidazoles

Ute Scheffer, Andreas Strick, Verena Ludwig, Sascha Peter, Elisabeth Kalden, and Michael W. Gbel

J. Am. Chem. Soc., **2005**, 127 (7), 2211-2217• DOI: 10.1021/ja0443934 • Publication Date (Web): 27 January 2005

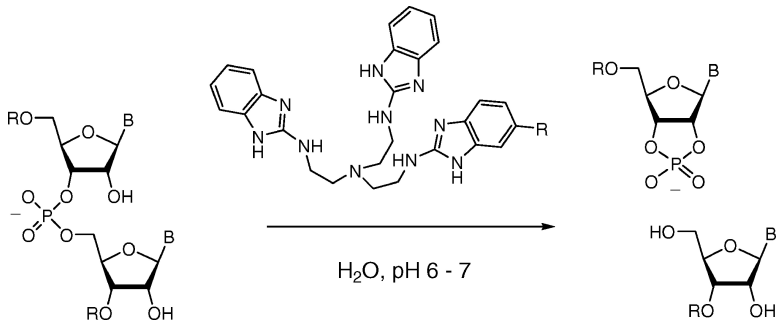

More About This Article

Additional resources and features associated with this article are available within the HTML version:

- Supporting Information
- Links to the 8 articles that cite this article, as of the time of this article download
- Access to high resolution figures
- Links to articles and content related to this article
- Copyright permission to reproduce figures and/or text from this article

View the Full Text HTML

Journal of the American Chemical Society is published by the American Chemical Society. 1155 Sixteenth Street N.W., Washington, DC 20036

J|A|C|S
ARTICLES
Published on Web 01/27/2005

Metal-Free Catalysts for the Hydrolysis of RNA Derived from Guanidines, 2-Aminopyridines, and 2-Aminobenzimidazoles

Ute Scheffer, Andreas Strick, Verena Ludwig, Sascha Peter, Elisabeth Kalden, and Michael W. Göbel*

Contribution from the Institute for Organic Chemistry and Chemical Biology, Goethe-University Frankfurt, Marie-Curie-Str. 11, 60439 Frankfurt am Main, Germany

Received September 15, 2004; E-mail: M.Goebel@chemie.uni-frankfurt.de

Abstract: 2-Aminopyridine and 2-aminobenzimidazole were chosen as structural analogues to substitute guanidinium groups in receptor molecules designed as phosphoryl transfer catalysts. Shifting the pK_a of the guanidinium analogues toward 7 was expected to raise catalytic activities in aqueous buffer. Although the pK_a's of both heterocycles are similar (6.2 and 7.0), only 2-aminobenzimidazole led to active RNA cleavers. All cleavage assays were run with fluorescently labeled substrates and a DNA sequencer. RNase contaminations would degrade RNA enantioselectively. In contrast, achiral catalysts such as **9b** and **10b** necessarily induce identical cleavage patterns in RNA and its mirror image. This principle allowed us to safely rule out contamination effects in this study. The most active catalysts, tris(2-aminobenzimidazoles) **9b** and **10b**, were shown by fluorescence correlation spectroscopy (FCS) to aggregate with oligonucleotides. However, at very low concentrations the compounds are still active in the nonaggregated state. Conjugates of **10b** with antisense oligonucleotides or RNA binding peptides, therefore, will be promising candidates as site specific artificial ribonucleases.

Introduction

The chemistry of artificial phosphodiesterases and ribonucleases is a challenging field of research due to the high kinetic stability of phosphodiester ions against nucleophilic attack.[1] This functional group is known for reaction barriers up to 100 kcal mol^{-1} in vacuo.[1d,2] The remarkable value results from charge repulsion, e.g., between dimethyl phosphate and the methoxide ion.[2b,c] In aqueous solution, the dipole moment of water efficiently stabilizes the transition state of phosphate substitution. This phenomenon, electrophilic catalysis, is predicted by calculations and observed in many experiments.[2b−e] Increased positive charge density further enhances the catalytic power of electrophiles. Accordingly, lanthanide ions are among the most successful artificial ribonucleases known today.[1b] In aqueous solution around pH 7, the dominant nucleophilic species are water and neutral hydroxy groups, respectively. General bases to activate nucleophiles and general acids to protonate leaving groups, therefore, may further contribute to phosphoryl transfer catalysis.[1c]

Some time ago, we have studied the catalytic influence of guanidinium ions on the reaction of catechol cyclic phosphate and phenylethanol in DMF (Scheme 1).[3a] Two guanidinium groups, when connected by appropriate spacers, showed significant cooperativity in this process. Interestingly, the substitution of guanidinium ions in compound **1b** by heterocyclic analogues (**2b**) led to a 10-fold rate increase (Chart 1). Comparable effects have been consistently observed in several reactions. The enhanced catalytic power of 2-aminoimidazolinium has been attributed to the increased acidity of this ion compared to guanidinium.[3b] Increased acidity reinforces hydrogen bonds with the substrate and improves transition state stabilization. In addition, it enables the cation to participate in general acid/base catalysis.[4]

Scheme 1

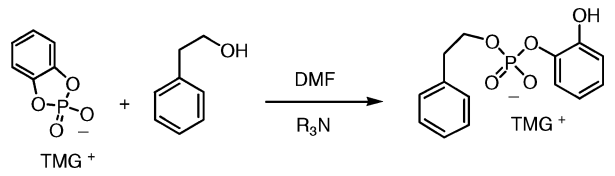

Bis(guanidinium) compounds have been described by several laboratories as useful phosphate receptors and transesterification catalysts in nonaqueous solution.[3,5] In water, however, high rate increases are rarely observed.[6] Furthermore, the rate advantage

(1) (a) Perreault, D. M.; Anslyn, E. V. *Angew Chem., Int. Ed. Engl.* **1997**, *36*, 432. (b) Trawick, B.; Daniher, A. T.; Bashkin, J. K. *Chem. Rev.* **1998**, *98*, 939. (c) Oivanen, M.; Kuusela, S.; Lönnberg, H. *Chem. Rev.* **1998**, *98*, 961. (d) Zhou, D.-M.; Taira, K. *Chem. Rev.* **1998**, *98*, 991. (e) Kuimelis, R. G.; McLaughlin, L. W. *Chem. Rev.* **1998**, *98*, 1027.

(2) (a) Lim, C.; Tole, P. *J. Am. Chem. Soc.* **1992**, *114*, 7245. (b) Dejaegere, A.; Karplus, M. *J. Am. Chem. Soc.* **1993**, *115*, 5316. (c) Dejaegere, A.; Liang, X.; Karplus, M. *J. Chem. Soc., Faraday Trans.* **1994**, *90*, 1763. (d) Yliniemela, A.; Uchimaru, T.; Tanabe, K.; Uebayasi, M.; Taira, M. *J. Am. Chem. Soc.* **1993**, *115*, 3032. (e) Taira, M.; Uchimaru, T.; Storer, J. W.; Yliniemela, A.; Uebayasi, M.; Tanabe, K. *J. Org. Chem.* **1993**, *58*, 3009. (f) Uchimaru, T.; Stec, W. J.; Taira, K. *J. Org. Chem.* **1997**, *62*, 5793.

(3) (a) Gross, R.; Dürner, G.; Göbel, M. W. *Liebigs Ann. Chem.* **1994**, 49. (b) Muche, M.-S.; Göbel, M. W. *Angew. Chem., Int. Ed. Engl.* **1996**, *35*, 2126. (c) Kurz, K.; Göbel, M. W. *Helv. Chim. Acta* **1996**, *79*, 1967.

(4) By proton inventory studies, it has been shown recently that even unmodified guanidinium ions are sufficiently acidic to protonate the dianionic phosphorane transition state or intermediate of phosphoryl transfer reactions: Piatek, A. M.; Gray, M.; Anslyn, E. V. *J. Am. Chem. Soc.* **2004**, *126*, 9878.

Chart 1. Structures of Compounds **1**−**10**

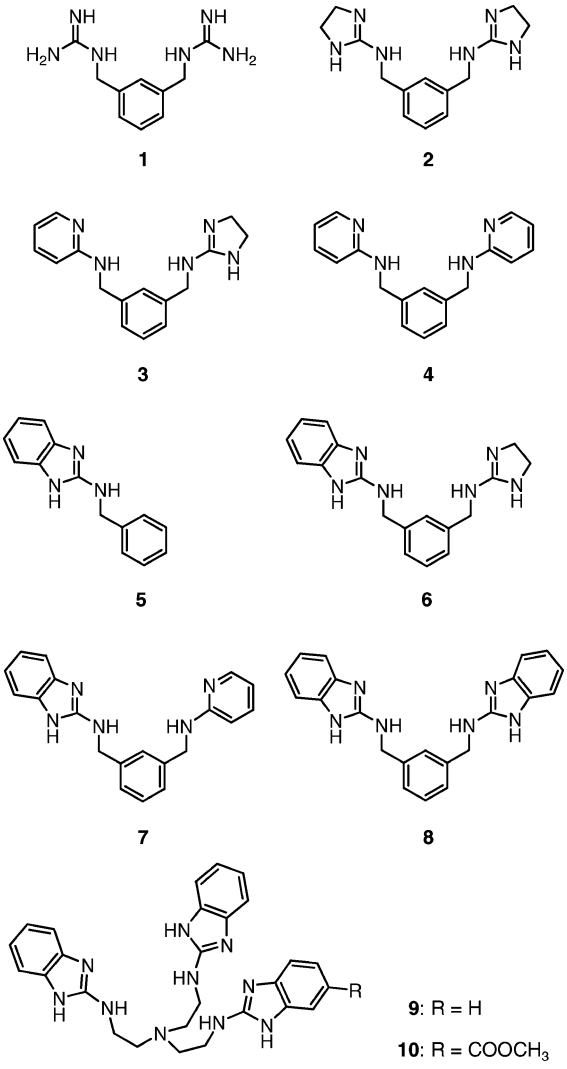

Scheme 2

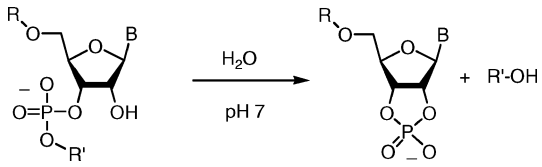

of compound **2b** over **1b** disappears when applied to RNA hydrolysis (Scheme 2). For an explanation, several factors have to be considered. First of all, ion pair stability is reduced by the solvent change from DMF to water. In addition, water itself is a good electrophile due to its high polarity making it difficult to surpass aqueous transition state solvation by guanidinium groups. Finally, the protonation equilibrium of guanidines in water is shifted toward the cation. Both compounds **1b** and **2b**, as a result, are not sufficiently acidic to participate in proton transfer steps. The remaining activity of **1b** and **2b** as pure electrophilic catalysts is too weak to generate important rate effects. We will show below that shifting the pK_a of the cationic groups toward 7 leads to promising synthetic RNA cleavers. Increasing the number of charged groups gives a further boost to catalytic power.

Results and Discussion

Synthesis of Catalysts. Derivatives of 2-aminopyridine were obtained by heating the diamine **11** with 2-bromopyridine **12**. Subsequent reaction with di-*tert*-butyl dicarbonate led to a mixture of bis-2-aminopyridine **4** (12%) and compound **13** (52%) that was transformed into product **3a** by reagent **14**[3b] (95%). 2-Aminobenzimidazoles are accessible by reaction of the corresponding amines with thiocarbonyl diimidazole followed by a second substitution with 1,2-phenylene diamine.[7] A thiourea is formed in this step. It undergoes smooth cyclization in the presence of HgO.[7,8] Thus, benzylamine **15** could be transformed into picrate **5a** in 49% total yield. Analogous procedures were used to prepare the catalyst picrates **6a** and **8a** as depicted in Scheme 3. In the case of compound **7**, the benzimidazole moiety could be attached by heating the amine precursor in the presence of 2-chlorobenzimidazole. However, this procedure required high reaction temperatures and led to products with insufficient yield and purity (20% after HPLC separation).

Tris(2-aminoethyl)amine **21** (TREN) has been often used as a building block in coordination chemistry. It also forms the framework of several anion receptors based on guanidines and ureas.[9] For the synthesis of compound **9a** (Scheme 4), TREN

(5) (a) Jubian, V.; Dixon, R. P.; Hamilton, A. D. *J. Am. Chem. Soc.* **1992**, *114*, 1120. (b) Jubian, V.; Veronese, A.; Dixon, R. P.; Hamilton, A. D. *Angew. Chem., Int. Ed. Engl.* **1995**, *34*, 1237. (c) Smith, J.; Ariga, K.; Anslyn, E. V. *J. Am. Chem. Soc.* **1993**, *115*, 362. (d) Perreault, D. M.; Cabell, L. A.; Anslyn, E. V. *Bioorg. Med. Chem.* **1997**, *5*, 1209. (e) Kato, T.; Takeuchi, T.; Karube, I. *J. Chem. Soc., Chem. Commun.* **1996**, 953. (f) Oost, T.; Filippazzi, A.; Kalesse, M. *Liebigs Ann. Recl.* **1997**, 1005. (g) Oost, T.; Kalesse M. *Tetrahedron* **1997**, *53*, 8421. (h) Zepik, H. H.; Benner S. A. *J. Org. Chem.* **1999**, *64*, 8080. Selected recent papers on guanidinium carboxylate recognition: (i) Schmuck, C.; Geiger, L. *J. Am. Chem. Soc.* **2004**, *126*, 8898. (j) Linton, B.; Hamilton, A. D. *Tetrahedron* **1999**, 6027. (k) Linton, B. R.; Goodman, M. S.; Fan, F.; van Arman, S. A.; Hamilton, A. D. *J. Org. Chem.* **2001**, *66*, 7313. (l) Zafar, A.; Melendez, R.; Geib, S. J.; Hamilton, A. D. *Tetrahedron* **2002**, *58*, 683. Crystal structure of the sulfate salt of bis(guanidinium) compound **1**: (m) Hutchings, M. G.; Grossel, M. C.; Merckel, D. A. S.; Chippendale, A. M.; Kenworthy, M.; McGeorge, G. *Cryst. Growth Des.* **2001**, *1*, 339. Crystal structure of 2-aminobenzimidazolium nitrate: (n) Bats, J. W.; Gördes, D.; Schmalz, H.-G. *Acta Crystallogr.* **1999**, *C55*, 1325.

(6) For a Zn^{2+}-bis(guanidinium) catalyst cleaving ApA, see: (a) Ait-Haddou, H.; Sumaoka, J.; Wiskur, S. L.; Folmer-Andersen, F. J.; Anslyn, E. V. *Angew. Chem., Int. Ed.* **2002**, *41*, 4014. RNA cleavers based on amines: (b) Yoshinari, K.; Yamazaki, K.; Komiyama, M. *J. Am. Chem. Soc.* **1991**, *113*, 5899. (c) Komiyama, M.; Yoshinari, K. *J. Org. Chem.* **1997**, *62*, 2155. (d) Verheijen, J. C.; Deiman, B. A. L. M.; Yeheskiely, E.; van der Marel, G. A.; van Boom, J. H. *Angew. Chem., Int. Ed.* **2000**, *39*, 369. (e) Petersen, L.; de Koning, M. C.; van Kuik-Romeijn, P.; Weterings, J.; Pol, C. J.; Platenburg, C.; Overhand, M.; van der Marel, G. A.; van Boom, J. H. *Bioconjugate Chem.* **2004**, *15*, 576. (f) Michaelis, K.; Kalesse M. *Angew. Chem., Int. Ed.* **1999**, *38*, 2243. (g) Michaelis, K.; Kalesse M. *ChemBioChem.* **2001**, *1*, 79. (h) Scarso, A.; Scheffer, U.; Göbel, M.; Broxterman, Q. B.; Kaptein, B.; Formaggio, F.; Toniolo, C.; Scrimin, P. *Proc. Natl. Acad. Sci. U.S.A.* **2002**, *99*, 5144. For imidazole based RNA cleavers see: (i) Beloglazova, N. G.; Fabani, M. M.; Zenkova, M. A.; Bichenkova, E. V.; Polushin, N. N.; Silnikov, V. V.; Douglas, K. T.; Vlassov, V. V. *Nucleic Acids Res.* **2004**, *32*, 3887. (j) Fouace, S.; Gaudin, C.; Picard, S.; Corvaisier, S.; Renault, J.; Carboni, B.; Felden, B. *Nucleic Acids Res.* **2004**, *32*, 151. For RNA cleaving peptides, see: (k) Mironova, N. L.; Pyshnyi, D. V.; Ivanova, E. M. In *Artificial Nucleases*; Zenkova, M. A., Ed.; Springer: Berlin, 2004; p 151.

(7) Perkins, J. J.; Zartman, A. E.; Meissner, R. S. *Tetrahedron Lett.* **1999**, *40*, 1103.

(8) Mohsen, A.; Omar, M. E.; Ragab, M. S.; Farghaly, A. M.; Barghash, A. M. *Pharmazie* **1976**, *31*, 348.

(9) For the corresponding tris(guanidine), see: (a) Dietrich, B.; Fyles, D. L.; Fyles, T. M.; Lehn, J.-M. *Helv. Chim. Acta* **1979**, *62*, 2763. (b) Pitsch, S.; Scheffer, U.; Strick, A.; Göbel, M. W. *Helv. Chim. Acta* **2003**, *86*, 3740. TREN derived urea derivatives as anion receptors: (c) Raposo, C.; Almaraz, M.; Martin, M.; Weinrich, V.; Mussons, M. L.; Alcazar, V.; Cruz Caballero, M.; Moran, J. R. *Chem. Lett.* **1995**, 759. (d) Werner, F.; Schneider, H.-J. *Helv. Chim. Acta* **2000**, *83*, 465. (e) Xie, H.; Yi, S.; Wu, S. *J. Chem. Soc. Perkin Trans. 2* **1999**, *12*, 2751. TREN derived urea derivatives as organic gelators: (f) de Loos, M.; Ligtenbarg, A. G. J.; van Esch, J.; Kooijman, H.; Spek, A. L.; Hage, R.; Kellogg, R. M.; Feringa, B. L. *Eur. J. Org. Chem.* **2000**, *22*, 3675. TREN derived guanidines as ligands for metal

Scheme 3. Synthesis of Compounds **3**−**8**

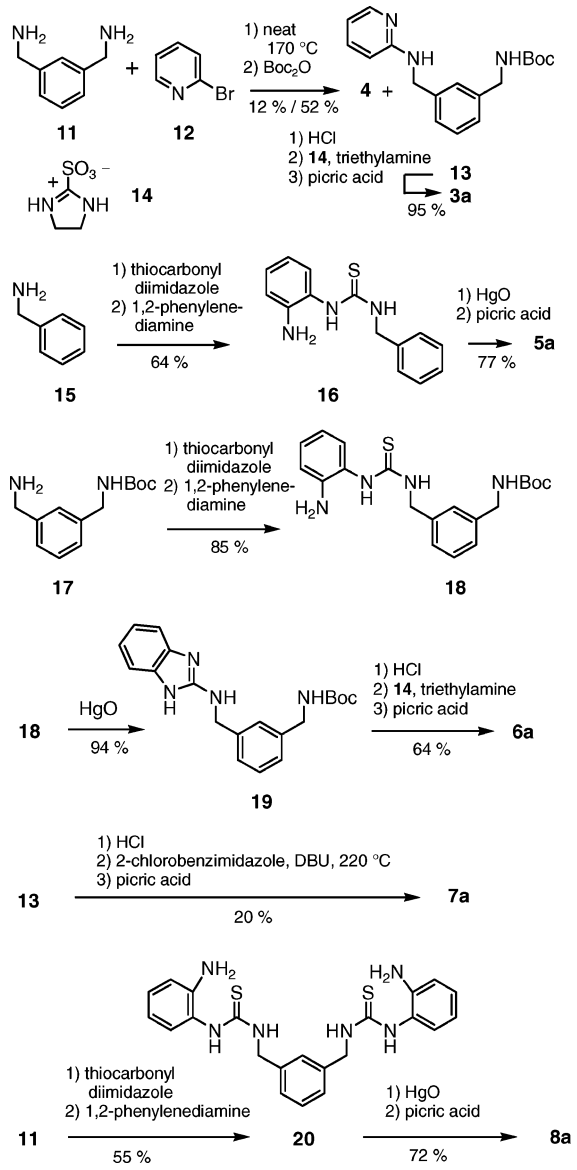

was transformed into thiourea **22** by addition to excess *o*-nitrophenylisothiocyanate (55%).[7,10] After hydrogenation of the nitro groups (**23**, 27%), HgO induced cyclization led to the final product **9** (64%). The analogous compound **10** was prepared from the Boc protected TREN derivative **24**. Compound **10** is equipped with an ester group to allow conjugation of RNA ligands in future studies. Stepwise reaction of **24** with thiocarbonyl diimidazole and compound **25** formed thiourea **26** (88%) which readily cyclized in the presence of HgO (97%). The resulting benzimidazole **27** could be converted into product **10** via addition of *o*-nitrophenylisothiocyanate, reduction, and ring closure as in the case of **9** (37% from **27**). Hydrochloride salts **3b**−**10b** were prepared from the corresponding picrates by filtration over ion-exchange resin. Acidity constants in 100 mM phosphate buffer, determined photometrically at 50 μM substrate concentrations, are summarized in Table 1. While titrations of

Scheme 4. Synthesis of Tris(benzimidazoles) **9** and **10**

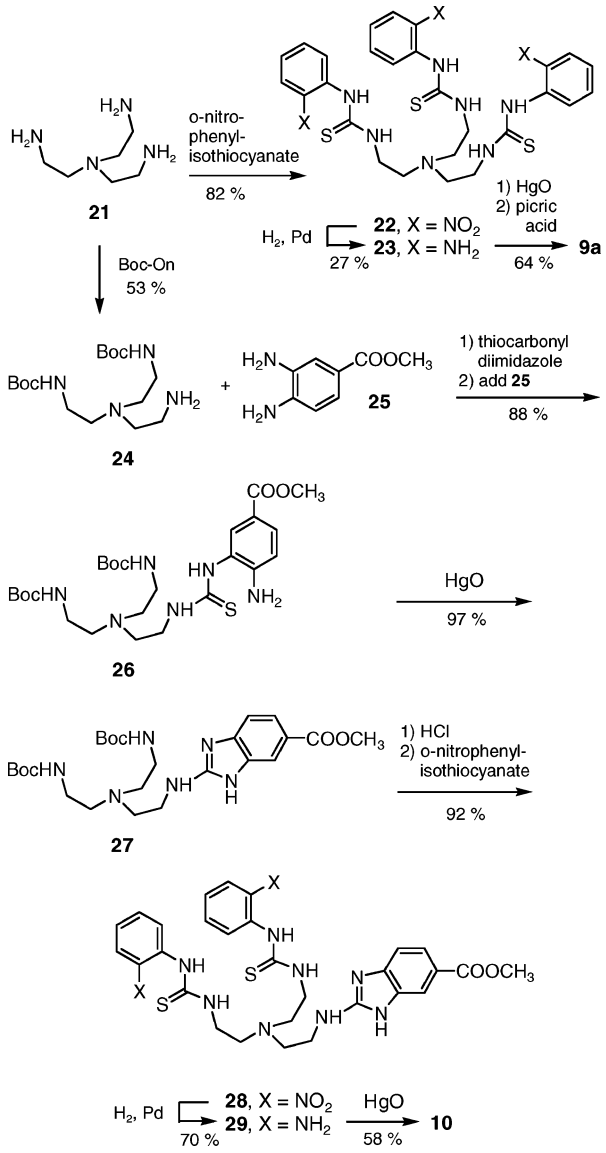

Table 1. Acidity Constants of Compounds **3b**−**8b**[a]

compound	pK_a	determined at λ [nm]
3b	6.2	250
4b	6.5	250
5b	6.9	288
6b	6.6	288
7b	7.1	288
8b	7.0	288
9b	n.d.	288

[a] Photometrically determined at 50 μM substrate concentration in 100 mM phosphate buffer. All data were averaged over a minimum of two experiments.

compounds **9** and **10** behaved well in acidic solution, nonreproducible effects occurred around pH 7 indicating some form of aggregation. Furthermore, absorption versus concentration curves did not fulfill Lambert−Beer's law under these conditions.

RNA Hydrolysis. DNA sequencers allow the online detection of fluorescently labeled oligonucleotides. Based on this technique we and others have studied the degradation[9b,11] or extension[12] of RNA chains. To achieve the best resolution of

ions: (g) Raab, V.; Kipke, J.; Burghaus, O.; Sundermeyer J. *Inorg. Chem.* **2001**, *40*, 6964. (h) Wittmann, H.; Raab, V.; Schorm, A.; Plackmeyer, J.; Sundermeyer, J. *Eur. J. Inorg. Chem.* **2001**, 1937. (i) Walther, M.; Wermann, K.; Görls, H.; Anders, E. *Synthesis* **2001**, 1327.

(10) Peyman, A.; Gourvest, J.-F.; Gadek, T. R.; Knolle, J. *Angew. Chem., Int. Ed.* **2000**, *39*, 2874.

Chart 2. Sequences of Oligonucleotides **30**−**35**

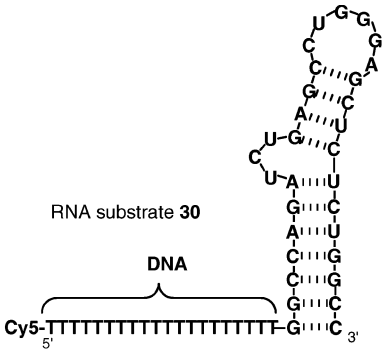

Cy5-T_{10}-ribo(CUAGCCGACUGCCGAUCUCGCUGACUGAC) 3'
RNA substrate **31**

Cy5-T_{10}-ribo(CUAGCCGACUGCCGAUCUCGCUGACUGAC)-T_4 3'
RNA substrate **32**

Cy5-T_{10}-*ent*-ribo(GGCCAGAUCUGAGCCUGGGAGCUCUCUGGCC)-T_4 3'
enantiomeric RNA **33**

Cy5-TTTTTTTTTTTTTTTTTTTTU 3' **34**

TGTGGAATTGTGAGCGGATA 3' **35**

all possible fragment bands, a short DNA spacer was placed between the fluorescent dye and the RNA part. The presence of very short fragments complicating the analysis is thus avoided. Two sequences were chosen as substrates: a 31mer hairpin structure derived from HIV-1 TAR (**30**) and a linear 29mer (**31**,[13] Chart 2). Four additional deoxynucleotides have been attached to the 3′ end of RNAs **32** and **33** to improve the separation of substrates and the longest degradation products. The RNA part of **33** represents the TAR sequence of **30** but was synthesized from enantiomeric nucleotides.[9b] DNA **34**, diluted with the unmodified DNA **35**, served as a dye-labeled, nondegradable oligomer for aggregation studies.

Special care was taken to avoid contaminations by natural ribonucleases. Since catalysts **3b**−**9b** could not be prepared under sterile conditions, their solutions were purified by ultrafiltration.[14] In a first set of experiments, all catalysts were tested at high concentrations (10 mM, 37 °C, see Figure 1 and Table 2). The limited solubility required pH 6.0 for compounds **3b** and **4b**. For other catalysts pH 7.0 was chosen. The degree of cleavage after incubation with **4b** for 20 h (<1% for **30** and 2% for **31**) was not much above the background level (<1% in most runs). More hydrolysis was seen with compound **3b** (4%/6%). Remarkably, the single benzimidazole unit of **5b** was sufficient to exceed these results: 13% of RNA **30** and 15% of **31** were hydrolyzed. While a second imidazolinium ion (**6b**) did not change the reactivity, an aminopyridine unit increased the catalytic power (**7b**). By far the highest rates of hydrolysis were obtained with bis(benzimidazole) **8b**. However, the latter experiment worked at the solubility limits of this compound.

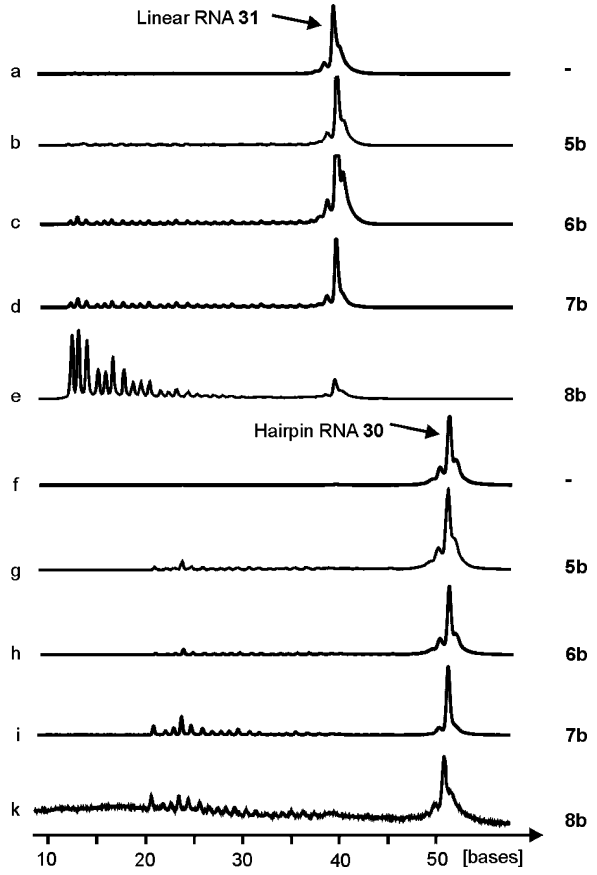

Figure 1. RNA cleavage induced by compounds **5b**, **6b**, **7b**, and **8b** at 10 mM catalyst concentration (120−140 nM RNA, 50 mM Tris-HCl pH 7.0, 0.01% SDS, 37 °C, 20 h).

Table 2. Catalyst Efficiency at 10 mM Concentration[a]

		% degradation	
compound	pK_a	linear RNA **31**	hairpin RNA **30**
3b	6.2	6[1]	4[1]
4b	6.5	2[1]	<1[1]
5b	6.9	15	13
6b	6.6	15	13
7b	7.1	31	31
8b	7.0	n.d.	86
36b		2.4	1.1
37b		1.3	3.4
38b		4.6	1.3
39b		5.2	2.3
		<1	<1

[a] 120−140 nM RNA, 50 mM Tris-HCl, pH 7.0 ([1]pH 6.0), 0.01% SDS, 37 °C, 20 h.

Excessive RNA precipitation was observed in several runs. The resulting poor signal-to-noise ratios made quantitative analysis in those cases impossible (see Figure 1, lane k). For the same reason, no data could be obtained for tris(benzimidazole) **9b**. To minimize the loss of labeled oligonucleotides by nonspecific hydrophobic interactions, we added 0.01% of sodium *n*-dodecyl sulfate (SDS) to the cleavage buffer.[15] A small set of amines (hydrochlorides of **36**−**39**, Chart 3) was tested as a control since RNA hydrolysis by NH_2 groups is a well documented phenomenon.[6b−h] Amine promoted degradation was

(11) (a) Gläsner, W.; Merkl, R.; Schmidt, S.; Cech, D.; Fritz, H.-J. *Biol. Chem. Hoppe-Seyler* **1992**, *373*, 1223. (b) Schmidt, C.; Welz, R.; Müller, S. *Nucleic Acids Res.* **2000**, *28*, 886.
(12) Hey, M.; Hartel, C.; Göbel, M. W. *Helv. Chim. Acta* **2003**, *86*, 844.
(13) Hall, J.; Hüsken, D.; Pieles, U.; Moser, H. E.; Häner, R. *Chem. Biol.* **1994**, *1*, 185.
(14) Podyminogin, M. A.; Vlassov, V. V.; Giegé, R. *Nucleic Acids Res.* **1993**, *21*, 5950.
(15) Santoro, S. W.; Joyce, G. F. *Proc. Natl. Acad. Sci. U.S.A.* **1997**, *94*, 4262.

Chart 3. Amines Tested in the RNA Cleavage Assay

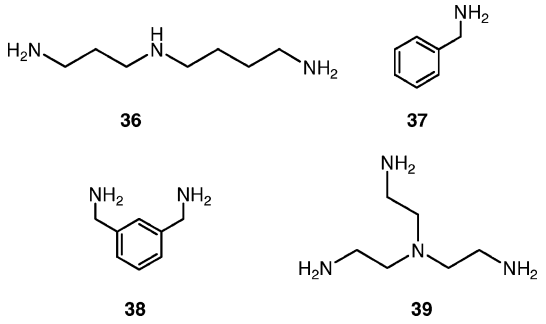

somewhat above the background level (<1%) but rarely surpassed 3% (see Table 2).

The most promising candidates (**5b**−**9b**) were then compared under conditions ensuring sufficient solubility (pH 6.0, 1 mM catalyst concentration). Among the biscationic compounds, again **8b** induced the highest cleavage rates. Combining three aminobenzimidazoles in structure **9b**, therefore, should lead to highly active catalysts. Indeed, almost complete hydrolysis of all RNA substrates was observed in the presence of **9b** (Figure 2, Table 3). The reaction is specific for RNA, since no degradation is seen in the DNA part of the substrates.

In these initial assays, compound **9b** clearly showed up as the most promising catalyst. The more detailed studies, therefore,

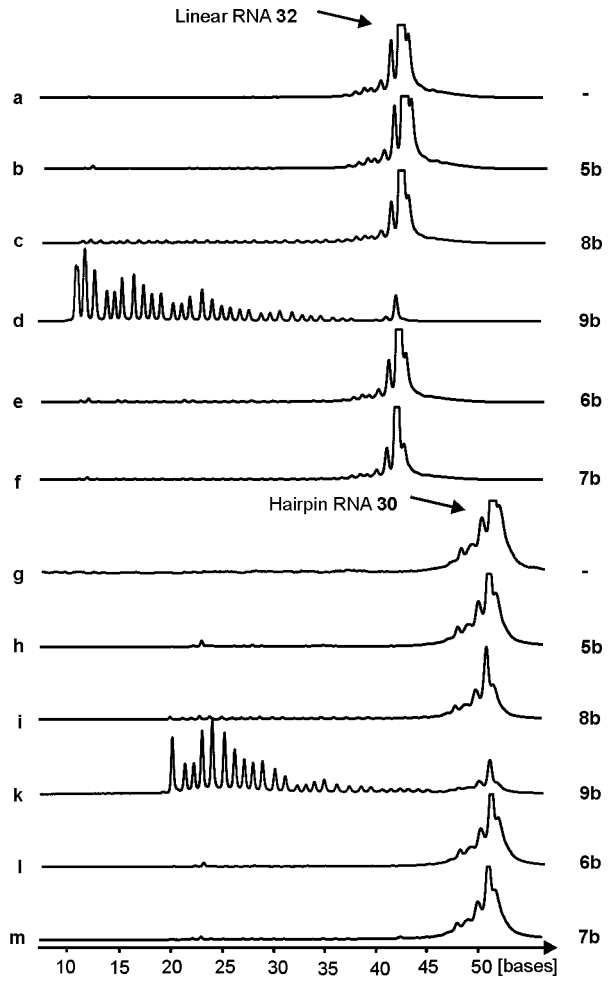

Figure 2. RNA cleavage induced by compounds **5b**, **6b**, **7b**, **8b**, and **9b** at 1 mM catalyst concentration (120−140 nM RNA, 50 mM Tris-HCl pH 6.0, 0.01% SDS, 37 °C, 20 h).

Table 3. Catalyst Efficiency at 1 mM Concentration[a]

		% degradation	
compound	pK_a	linear RNA **32**	hairpin RNA **30**
5b	6.9	4.8	2.4
6b	6.6	4.6	3.0
7b	7.1	4.5	3.2
8b	7.0	23.1	15.3
9b	n.d.	92.9	87.6

[a] 120−140 nM RNA, 50 mM Tris-HCl, pH 6.0, 0.01% SDS, 37 °C, 20 h. All data were averaged over two experiments.

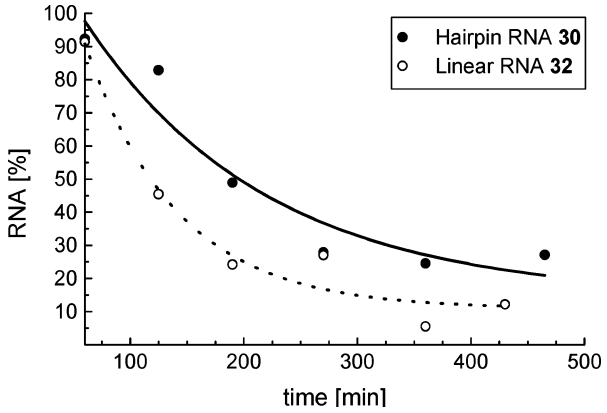

Figure 3. Time-dependent RNA cleavage in the presence of 1 mM catalyst **9b** (120−140 nM RNA, 50 mM Tris-HCl pH 6.0, 0.01% SDS, 37 °C).

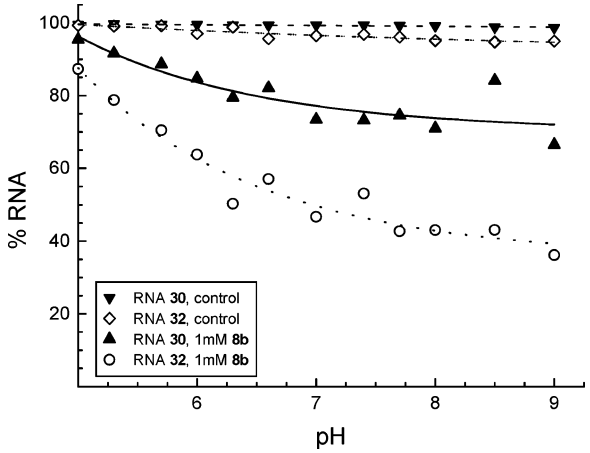

Figure 4. pH dependent RNA cleavage at 1 mM concentration of **8b** (120−140 nM RNA, 50 mM Tris-HCl, 0.01% SDS, 37 °C, 20 h).

concentrated on **9b** and its analogue **10b**. The time course of RNA hydrolysis was studied next. The decrease of substrate concentration versus time at 1 mM **9b** and pH 6.0 could be fitted to a first-order rate law (Figure 3). The resulting half-lives are 120 min for the linear RNA **32** and 200 min for the TAR analogue **30**, respectively. This corresponds to a formal first-order rate constant of 3.3×10^{-6} s^{-1} for a mean phosphodiester linkage in substrate **32** (29 susceptible bonds).

The pH is expected to influence the rates of benzimidazole induced RNA hydrolysis. Systematic studies with compound **9b** were hampered by the limited solubility above pH 7. However, at 1 mM concentration they could be carried out with bis(benzimidazole) **8b**. As shown in Figure 4, cleavage rates increase steadily with increasing pH. At any pH, they are far above background levels. pH versus rate curves may show the protonation state of **8b** or **9b** relevant to catalysis. The

Table 4. RNA Cleavage as a Function of [**9b**][a]

concentration **9b** [μM]	% degradation linear RNA **32**	% degradation hairpin RNA **30**
250	87.4	48.7
200	85.6	44.8
150	63.3	27.1
120	60.3	26.7
100	16.6	8.5
80	6.2	6.4
60	3.9	6.5
40	5.2	5.2
20	6.3	7.7
10	4.1	1.1

[a] RNA cleavage in the presence of 0.01% SDS. 120−140 nM RNA, 50 mM Tris-HCl, pH 6.0, 37 °C, 20 h.

requirement for such conclusions, however, would be the absence of complicating effects such as pH dependent aggregation. With the nonideal behavior of **9b** in mind, mechanistic interpretations of Figure 4 are highly dangerous (see below).

Table 4 shows the dependence of the total amount of RNA cleavage on catalyst concentration. The reaction is still fast at [**9b**] = 250 μM. At concentrations around 100 μM, a sudden decrease of cleavage occurs. Significant hydrolysis above background levels can be observed at catalyst concentrations as low as 20 μM. While the specific numbers in Table 4 are taken from a single dilution experiment and reflect the statistical error of the method, several repetitions of the whole dilution series could reproduce the sudden rate decrease below 100−150 μM. Essentially the same was seen with catalyst **10b**. Interestingly, the cleavage pattern induced by compounds **9b** and **10b** does not reflect the secondary structure of the TAR model **30** (see Figure 2, lane k). When repeated with the enantiomeric RNA **33**,[9b] the total amount of degradation at each catalyst concentration and the cleavage pattern were indistinguishable from the data produced with natural RNA **30**. At catalyst concentrations below 100 μM, however, some experiments with natural RNA **30** exhibited preferential cleavage after pyrimidines. This was never observed with enantiomeric substrate **33** and can only be explained as a minor contamination effect.[9b]

Relevance of Aggregation for the Activity of Catalysts 9b and 10b. The idea that aggregation phenomena involving tris(benzimidazole) catalysts and RNA may be crucial for the interpretation of cleavage data was triggered by two observations: the deviation of Lambert−Beer's law and the denaturation of RNA secondary structure. Fluorescence correlation spectroscopy (FCS) is a highly sensitive method for the detection of aggregates.[16] Thus, we have determined the diffusion time of the dye-labeled DNA **34** by FCS as a function of catalyst concentration and the presence of further additives. A nondegradable oligonucleotide was chosen to avoid time dependent effects caused by substrate hydrolysis. In Tris buffer pH 6.0 containing 0.01% sodium *n*-dodecyl sulfate (SDS) and low concentrations of **10b**, the diffusion time of **34** was 150−180 μs (24 °C), consistent with the molecular mass of 7.3 kDa. The data could be fitted to a one-component model. In contrast, with catalyst concentrations above 100 μM, large aggregates containing several copies of **34** appeared. As shown in Figure 5, a good

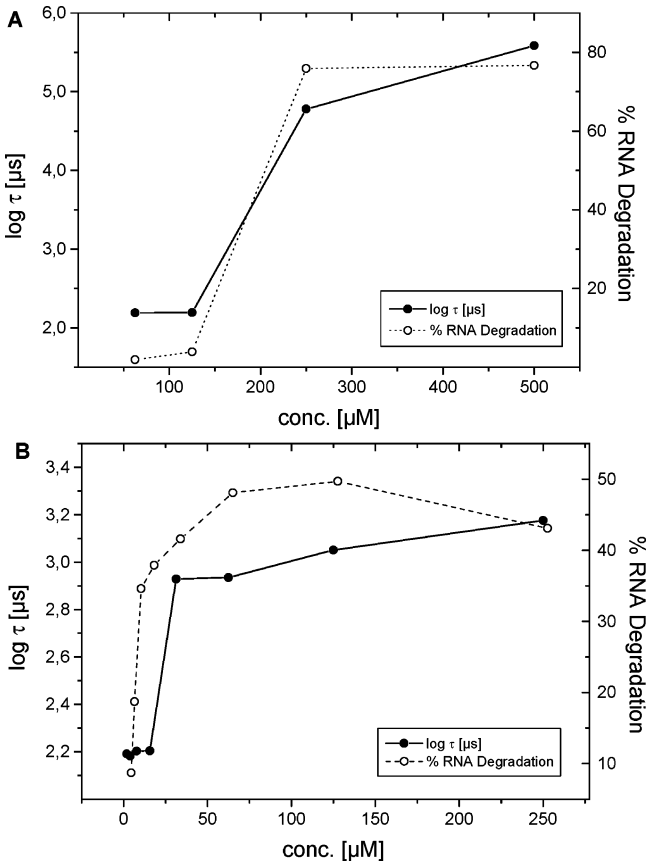

Figure 5. As detected by FCS, the presence of detergents has a critical influence on the aggregation of catalysts **9b** and **10b**. (A) 50 mM Tris-HCl pH 6.0, 0.01% SDS. (B) 50 mM Tris-HCl pH 6.0, 0.01% Triton X-100. Aggregation correlates with RNA cleavage yields. Left ordinate: diffusion time of oligonucleotide **34** (25 nM **34** + 175 nM **35**). Right ordinate: percentage of cleaved RNA **33** (150 nM).

correlation exists between cleavage of enantio-RNA **33** and aggregation of DNA **34**. However, when SDS was replaced by the nonionic detergent Triton X-100 (0.01%, 160 μM), aggregates of **34** could be seen at concentrations of **10b** as low as 4 μM. With Triton, no sudden catalyst deactivation below 100 μM occurs (Figure 5). When surfactants were completely omitted, the critical value of [**10b**] leading to aggregation of **34** again is 4 μM. These strange looking results are easily explained by noting that 0.01% SDS corresponds to 350 μM, a value far below the critical micelle concentration of 8 mM but equaling the concentration of benzimidazole units when [**9b**] or [**10b**] is 117 μM. In the final experiment, therefore, aggregation of **34** as a function of [**10b**] was studied in the presence of variable SDS concentrations. In all cases, aggregates of **34** disappeared when the point of equivalence between the anionic surfactant and the benzimidazole units was reached. It is our current view that both catalysts **9b** and **10b** self-assemble at pH 6.0 and concentrations down to 4 μM independently from the presence of nucleic acids. This is supported by finding identical aggregation thresholds with 25 nM DNA **34** alone or a mixture of 25 nM **34** plus 175 nM unlabeled DNA **35**. Nonionic surfactants, added to minimize unspecific hydrophobic interactions, interfere neither with this process nor with RNA binding to such aggregates. SDS, in contrast, may not influence the assembly of **9b** or **10b**, but it binds to the aggregates due to the combination of negative charge and hydrophobicity thus

(16) Müller, J.; Chen, Y.; Gratton, E. *Methods Enzymol.* **2003**, *361*, 69.

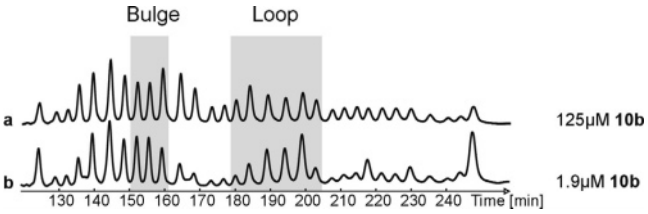

Figure 6. Degradation of hairpin RNA **33** induced by catalyst **10b** in the nonaggregated state at low concentrations. The cleavage pattern is consistent with the secondary structure shown in Chart 2.

preventing the interaction with oligonucleotides. The nonideal nature of the RNA-catalyst solutions has to be kept in mind to avoid misinterpretation of data (e.g., the pH dependency shown in Figure 4).

A central question remains: if RNA cleavage mainly correlates with aggregated forms of compound **9b** or **10b**, what can be expected for the catalytic activity of conjugates with antisense oligonucleotides or RNA binding peptides acting as single molecules? Figure 6 compares the degradation of the enantio-TAR model **33** at 125 μM and 1.9 μM concentrations of **10b** without any surfactant. In contrast to Figure 2 (lane k), the cleavage pattern starts to reflect the TAR secondary structure. At [**10b**] = 1.9 μM, a strong differentiation between nucleotides around the bulge, the loop, and the double helical parts is seen. Analogous assays with natural RNA **30** led to identical cleavage patterns. 20% of RNA **33** are degraded within 20 h (10% cleavage at [**10b**] = 0.9 μM) thus demonstrating the catalytic activity of tris(benzimidazoles) in the nonaggregated state.

Conclusions

The online detection of fluorescently labeled oligoribonucleotides allowed the precise and convenient characterization of RNA cleaving catalysts. By comparing reactions of naturally configurated and enantio-RNA, compelling evidence was found to rule out contamination effects that may corrupt the cleavage assays. Of all compounds tested, derivatives of 2-aminobenzimidazoles turned out to be powerful RNA cleavers. When compared with guanidines, the increased reactivity can be attributed to the pK_a change from 14 to 7. It is more difficult to explain the failure of the 2-aminopyridines **3** and **4**. With pK_a's around 6.2, these heterocycles are good candidates for general acid/base catalysis. In contrast to all other guanidinium analogues present in compounds **1**−**10**, the exocyclic C−N bond does not represent a local C_2 axis. Arguing by analogy with peptide bonds, the *Z* conformation should be preferred (Figure 7, amino N−H antiperiplanar to the C=N bond).[17] It is also

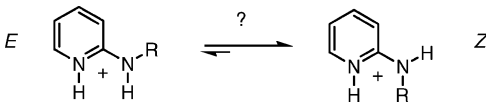

Figure 7. Conformers of protonated 2-aminopyridines.

known that *N*-substituted guanidinium ions form stable ion pairs only when they can offer two parallel N−H bonds to the guest (corresponding to "*E*" in Figure 7).[5j] Thus the ability to form undisturbed ion pairs between phosphate and heterocycle may be decisive for efficient acid/base catalysis. Unfavorable conformational equilibria could also account for the moderate and unpredictable transphosphorylation activities of some *N*-substituted guanidinium compounds.[5h]

The tris(2-aminobenzimidazoles) **9b** and **10b** proved to be among the most efficient metal free catalysts for RNA cleavage. At 1 mM catalyst concentration, the half-life of RNA compares well with the data of many metal complexes. As shown by fluorescence correlation spectroscopy, however, the active species under those conditions are aggregates of substrate and catalyst leading to denaturation of RNA secondary structure. Aggregation critically depends on the nature and concentration of further additives such as SDS. Compound **10b**, when tested at very low concentration, was shown to be active in the nonaggregated state as well. Conjugates of **10b** with sequence specific RNA ligands, therefore, have good prospects of success. The benzimidazole catalyzed hydrolysis is specific for RNA. Hence the overall mechanism must involve nucleophilic attack by 2′ hydroxy groups. Unfortunately, catalyst aggregation prevents further mechanistic insight from pH versus rate correlations. Such experiments will be accessible with oligonucleotide conjugates of **10b** in hand. Apart from the synthetic tasks, future work will try to dissect the different mechanistic aspects of aminobenzimidazole catalysis.

Acknowledgment. This paper is dedicated to the memory of Professor Jacques H. van Boom (1937−2004). Financial support by the European Community is gratefully acknowledged (European Network on the Development of Artificial Nucleases, HPRN-CT-1999-00008). We also would like to thank Prof. Stefan Pitsch, EPFL Lausanne, for providing us with a sample of enantiomeric RNA **33**.

Supporting Information Available: Experimental details, spectroscopic and analytical data for all new compounds. Figure S1: titration curve to determine the pK_a of compound **5b**. Figure S2: RNA cleavage induced by amines **36**−**39**. Figure S3: Time-dependent RNA cleavage in the presence of 1 mM catalyst **9b**. Table S1: diffusion times (FCS) of oligonucleotide **34** as a function of different additives. This material is available free of charge via the Internet at http://pubs.acs.org.

JA0443934

(17) Neutral 2-alkylaminopyridines normally adopt the *E* conformation, especially when bound to guest molecules such as carboxylic acids. Conformational polymorphism due to *E*/*Z* isomerization, however, is known from 2-arylaminopyridines: Bensemann, I.; Gdaniec, M.; Polonski, T. *New J. Chem.* **2002**, *26*, 448.